Climate signals recorded by Picea wilsonii tree-ring density over 220 years in the eastern section of Qilian Mountain, China

Jing Zhang
Inner Mongolia Agricultural University
Long Ma
malong4444333@163.com
Inner Mongolia Agricultural University
Tingxi Liu
Inner Mongolia Agricultural University
Bolin Sun
Inner Mongolia Agricultural University
Yingnan Wei
Inner Mongolia Agricultural University
Ziyue Zhang
Inner Mongolia Agricultural University

Research Article

Keywords: Eastern section of the Qilian Mountains, maximum latewood density, temperature reconstruction, dendroclimatology

Posted Date: March 11th, 2024

DOI: https://doi.org/10.21203/rs.3.rs-3998724/v1

Additional Declarations: No competing interests reported.

Climate signals recorded by *Picea wilsonii* tree-ring density over 220 years in the eastern section of Qilian Mountain, China

Jing Zhang, Long Ma*, Tingxi Liu, Bolin Sun, Yingnan Wei, Ziyue Zhang

Abstract: Global climate change has had a profound impact on the ecological environment and economic and social development. Therefore, research revealing the pattern of climate change over a long historical period is urgently needed. This paper analyses and studies the characteristics of climate change in the typical area of the eastern Qilian Mountains (Xinglongshan area) over more than two centuries using the chronological data of the maximum latewood density of *Picea wilsonii* in this area. Correlation analysis of the modern hydroclimatic data revealed that there was a significant positive correlation between the chronology and the mean annual temperature ($r = 0.77$, $P < 0.001$). Based on these data, we reconstructed the mean annual temperature of the study area for the period of 1801–2020. Characteristic analysis revealed that the reconstruction results of the mean annual minimum temperature are reliable. The study area has experienced 3 warm periods and 3 cold periods in the past 220 years, during which the cold period in the 19th century and the warm period in the 20th century were both consistent with recorded historical data. The cycle analysis results showed that the reconstructed mean annual temperature series exhibited cycle distribution characteristics of 11~16a, 36~45a, and 65~70a. In addition, large-scale spatial correlation analysis revealed that the reconstructed series could also reveal the climate change characteristics of the area around Xinglong Mountain. The mean annual temperature series for typical areas in the eastern section of the Qilian Mountains reconstructed in this paper reveal the climate change characteristics of this area during the historical period and provide references for global climate change studies.

Keywords: Eastern section of the Qilian Mountains; maximum latewood density; temperature reconstruction; dendroclimatology

Since the Industrial Revolution, the world has experienced climate change characterized by global warming. An increase in the global average temperature is accompanied by the frequent occurrence of extreme climatic events, such as snowmelt and glacial retreat, which have presented enormous threats and challenges to human survival and development (Hennessy et al.2022; Nunes et al.2022). According to China's climate change assessment report(Chao et al.2023), against the background of climate warming, the frequency and intensity of extreme climate events in China are significantly increasing, which has had a profound impact on China’s economic and social development, water resources, and ecological environment(He et al.2019). Climate change studies are a research hotspot in modern society (Yang et al.2021). Most meteorological stations in western China were established after the 1950s, which hindered the assessment of current climate change characteristics and patterns from a long-term perspective. However, tree rings can be used accurately reconstruct climates with strong continuity and high resolution, and they provide a geographic distribution. Therefore, the extensive range and good replication of meteorological data(Uttam et al.2023; Zachary et al.2022) are widely used in climate change studies over long historical periods(Chen et al.2023).

The Qilian Mountains are approximately 85 km long from east to west. These mountains are in the arid and semiarid region at midlatitudes. They are part of the famous high mountains in Northwest China. This area is affected by the summer monsoon near the end of its cycle, and the area is very sensitive to climate change. Therefore, the Qilian Mountains are considered to be one of the key regions for the study of dendroclimatology (Wang et al.2018; Xia et al.2017). The Xinglong Mountains, located in the eastwards extension of the Qilian Mountains, are a typical area in the eastern monsoon region. These mountains are located at the westernmost edge of the eastern monsoon region. With the influence of the confluence of species, the ecological environment has become extremely sensitive and fragile, and since climate reconstruction results have been lacking throughout the country’s long history, it is necessary to perform dendrochronology research here. At present, tree-ring climatology studies in typical areas of the eastern Qilian Mountains have focused mainly on tree-ring width; for example, one study showed that there is a significant negative correlation between the chronology of tree-ring width and temperature in this area(Jiao et al.2021; Liu et al.2021; Zhang et al.2011). These findings indicate that a continuous increase in temperature can inhibit the growth and development of plants. In addition, to analyse the changes in wetting and drying in this area, the millennial scale precipitation and drought indices reconstructed using the tree ring width chronology was analysed(Jiao et al.2021; Tian et al.2012; Zhang et al.2021). The results showed that tree growth was limited by drought stress, and the growth of the plants significantly decreased. There are relatively few studies using the maximum latewood density (MXD) of tree rings to reconstruct the hydrometeorological elements in this area, so it is necessary to use this tree ring indicator to develop relevant studies.

As an important parameter of tree rings, the MXD has a strong ability to record the mean temperature of trees growing in arid and semiarid areas (Esper et al.2018; Gou et al.2023; Timothy et al.2004). In comparison to more extensive climate reconstructions based on the mean width chronology, the MXD record usually contains less biological memory(Hartl et al.2022) and can better reconstruct the temperature and provide more accurate temperature change trends(Franke et al.2013); the MXD chronology is useful for preserving climate change throughout history; therefore, the reconstructed data that use this indicator can be used to assess volcanic activity(Briffa et al.2019), sunspot movement(Luckman et al.2005), greenhouse gases(Buntgen et al.2011)**Error! Reference source not found.** , or even orbital drive(Zheng et al.2023) impacts on climate change. Therefore, in this study, the typical area of the eastern section of Qilian (Xinglong Mountain area) was used as the study area for carrying out tree-ring climatology studies with the MXD of tree rings to fill the research gap on this tree-ring indicator and to accurately determine the trend and characteristics of temperature variation in the eastern section of the Qilian Mountains against a long-term historical background.

In summary, the purposes of this study are described as follows: (1) to establish a tree-ring MXD chronology for the eastern extension of the Qilian Mountains to determine the response relationship between the MXD chronology and climatic factors, (2) to reconstruct the chronology of the past 220 years in the study area, and (3) to analyse the change pattern of the reconstructed series of climatic elements in the past long historical period.

1. Materials and methods

1.1 Overview of the study area

The study area is located deep in the hinterland of East Asia in the Xinglong Mountain National Nature Reserve in Yuzhong County, Lanzhou city, Gansu Province. Xinglong Mountain is part of the eastern extension of the Qilian Mountain system, the mountain is about 37 kilometres long and 17 kilometres wide, the terrain is high in the south and low in the north, with an elevation of between 2000 and 3600 meters. Xinglong Mountain is rich in forest resources, of which the spruce forests are the key objects of protection, with a canopy density between 0.7 and 0.8. The study area is at the westernmost end of the eastern monsoon region, i.e., the end of the monsoon region. It also has a significant continental climate with four distinct seasons and heat and precipitation in the same season. The frequency of precipitation is uneven and mostly concentrated between July and September, and precipitation accounts for approximately 55% of the annual precipitation (based on the data from the Yuzhong Meteorological Station, the data are from the National Meteorological Information Center http://data.cma.cn/).

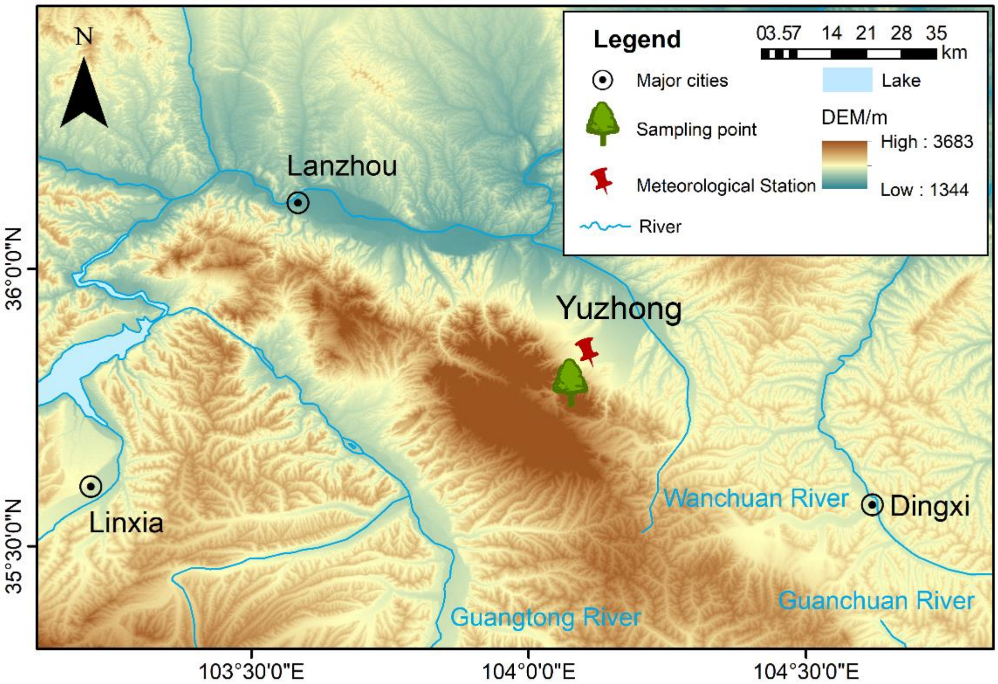

Figure 1 Overview of the study area

1.2 Tree-ring sample collection and chronology construction

Picea wilsonii is a tree plant of the genus Picea in the family Pinaceae that is mainly distributed in Inner Mongolia, Shaanxi, and Gansu provinces. This species often grows in areas at an altitude of 1400~2800 m; it is a photophilic plant, tolerates little shade, and thrives in a cool climate. It is suitable for growing in neutral, acidic or slightly calcic soils (Wang et al.2017). The sampling standards of the International Tree-Ring Data Bank (ITRDB) were strictly followed. Sixty sample cores from 30 trees were collected in September 2021 at an average altitude of 2280 m along Xinglong Mountain. The sampling cores were numbered, placed in a perforated ventilated PVC pipe and then brought indoors to dry naturally. After the sample core was completely dry, it was polished with sandpaper from coarse to fine grains until the surface of the sample core was smooth, and even cross-dating was performed by WinDENDRO software (accuracy: 0.001 mm). Then, the COFECHA program (Holmes et al.1983) was used to check the cross-dating quality, and the sample cores with poor quality and large differences from the main sequence were excluded. Finally, 56 sample cores from 30 trees were selected for tree-ring density analysis. The sample core was cut into thin slices with a thickness of 1.00±0.02 mm with a rotary slicer (Mcllwain). The thin slices were scanned by X-ray, and density analysis was performed on the X-ray film using tree-ring density analysis software (WinDENDRO Density 2022) to determine the density of each X-ray film. Seven tree ring parameters were employed in this study (mean tree ring width, earlywood width, latewood width, average earlywood density, average latewood density, minimum earlywood density, and MXD).

The MXD indicator was detrended using the polynomial function method(Cook et al.1994) in the ARSTAN procedure(Cook et al.1986), and the detrended results were synthesized by the biweight mean method to obtain the MXD chronology. Subsample signal strength (SSS) is a parameter used to determine the start year of a chronology. Generally, the first year with SSS>0.800 is taken as the starting year of the chronology. We used statistical feature values, such as correlation coefficients, to assess the quality of the chronology.

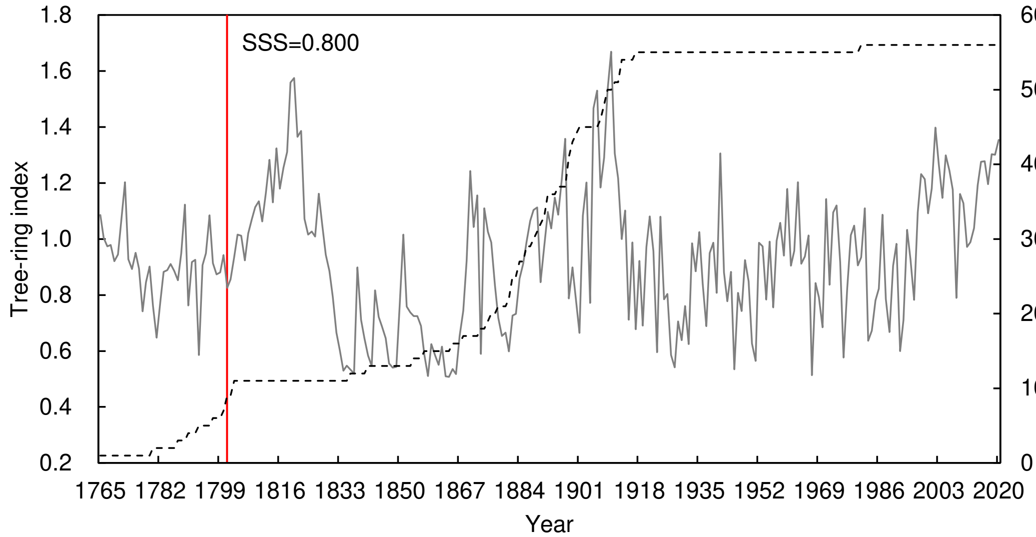

Figure 2 Chronological table and sample sizes of *Picea wilsonii* MXD in the Xinglong Mountains area, China

1.3 Climatic data

In this study, annual and monthly data on average temperature, average minimum temperature, average maximum temperature and average precipitation were collected from 1951 to 2016 at the Yuzhong meteorological station (35°52′N, 104°8′E, 1874 m above sea level). Data were obtained from the China National Meteorological Information Center (http://data.cma.cn/).

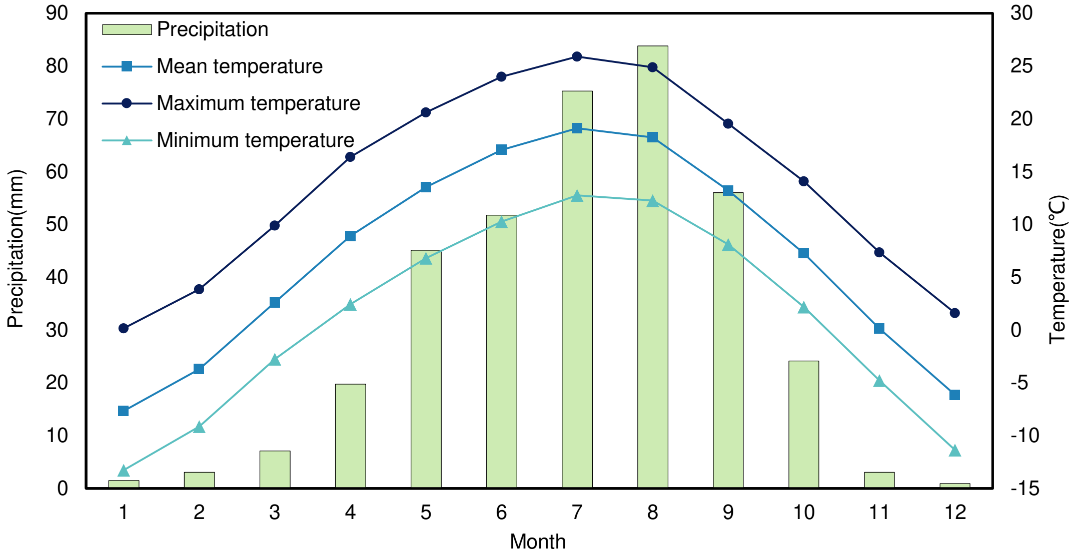

Figure 3 Monthly means with 3 types of temperatures and a distribution map of precipitation at the Yuzhong meteorological station from 1951 to 2020

1.4 Data analysis

(1) Using the Pearson correlation method(Keyimu et al.2020) , the correlation between the above meteorological data and the MXD chronology was analysed.

(2) Using a linear regression model(Liu et al.2019), a reconstruction equation was created as follows:

$$y = ax_i + b$$

where x_i is the tree ring density chronology, y is the reconstructed climatic factor, and a and b are the coefficients in the equation.

(3) The split–sample calibration test was used(Wang et al.2021). The completeness and reliability of the model were tested. This test is a commonly used method in tree ring meteorology. The statistical parameters used included the correlation coefficient (r), R-squared (R^2), sign test (ST), and reduction error analysis (RE), effectiveness coefficient test (CE), and product mean test (t).

(4) The Mann–Kendall nonparametric statistical method was used(Zhao et al.2021) for a temperature abrupt change test on the reconstructed temperature series.

(5) The variation coefficient C_V was used to represent the severity of the temperature change(Wang et al.2022), and the calculation formula is given as follows:

$$C_V = \left|\frac{SD}{MN}\right|$$

where SD is the standard deviation and MN is the mean value; a larger value of C_V indicates more severe temperature change.

(6) The mean and standard deviation (σ) of the reconstructed series are known. The years with temperatures higher than the mean+σ are defined as warmer years, and the years with temperatures lower than the mean−σ are defined as colder years. The year +1.5σ is defined as an extremely warm year, and the year with temperatures lower than the mean−1.5σ is defined as an extremely cold year.

$$\sigma = \sqrt{\frac{1}{N}\sum_{i=1}^{N}(X_i - \mu)^2}$$

where σ is the standard deviation, X_i is the corresponding temperature in the i-th year, μ is the mean value, and N is the number of samples (numbers).

(7) Morlet wavelet analysis was performed using MATLAB software(Venugopal et al.1996) to explore the change period and specific distribution age of the reconstructed series.

2 Results and analysis

2.1 Analysis of the chronological characteristics of tree rings with MXD

Table 1 shows the statistical feature values of the standardized chronology obtained from the analysis of the ARSTAN program. The first-order autocorrelation coefficient (Rac) can reflect the effect of climatic elements on the radial growth of trees in the current year, and the first-order autocorrelation coefficient of the MXD chronology is at the medium level. The results indicated that the hydroclimatic elements in the Xinglong Mountains area in the previous year had a certain continuous influence on the growth of *Picea wilsonii* in that year(Khasanov et al.2021). A higher mean sensitivity (MS) indicates that the MXD chronology contains more climate change information; thus, the reliability of reconstructing past climate change is also greater. Additionally, there are synchronous changes in the sample series. A larger value indicates stronger synchronization of the sample series and a stronger restriction of hydroclimatic elements on tree growth. The MXD chronology is strong in this respect, indicating that the MXD year can reflect more hydroclimatic signals. Based on the calculation of subsample signal strength (SSS), the years used by the MXD chronology to reconstruct past hydroclimatic elements are 1801~2020 AD.

Table 1 Statistical indicators and values of the MXD chronology in the Xinglong Mountain area

Statistical parameter	T/C	MS	SD	Rac	PCI	SNR	Rbt	$Y/C_{sss>0.80}$
MXD	30/56	0.498	0.325	0.311	54.7%	43.4	0.193	1801/2

Note: *T/C* tree (*T*)/core tree (*C*), mean sensitivity of *MS*, standard deviation of *SD*, first-order autocorrelation coefficient of *Rac*, $Y/C_{sss>0.80}$ (first-year and year when subsample signal intensity >0.80), *SNR* signal-to-noise ratio, *Rbt* inter-tree mean correlation coefficient, and *PCI* first eigenvector percentage.

2.2 Relationships between tree radial growth and climate

The 1951–2020 tree-ring MXD chronology data and instrumental data were used in this study. Pearson correlation analysis was performed to investigate the response of the tree density indicator to climatic factors. The results revealed that there was a strong positive correlation between the MXD chronology and the three temperature types at the interannual scale (P<0.001), and the correlation with the mean temperature was (r =0.770, P<0.001) >mean maximum temperature>mean minimum temperature. Similarly, the magnitude of the response to the precipitation factor over the same period was weak. Failing into the 95% confidence level, precipitation had a relatively nonsignificant limiting effect on the latewood density of *Picea wilsonii*. In terms of seasons, the three types of temperature had certain effects on tree growth, and the correlation coefficients in summer and autumn both passed the 0.05 significance level. The MXD chronology had a weak relationship with the three types of temperature responses from October to February, and the correlation coefficients did not reach the 95% confidence level. The three types of temperatures in the remaining months were significantly positively correlated with the chronology (P<0.05). The correlation on the scale did not pass the 0.05 significance level, again demonstrating that precipitation is not the main limiting factor for tree growth. In summary, temperature plays an important role in the growth process of *Picea wilsonii*, with a strong correlation occurring on an annual scale and revealing the most significant mean annual temperature.

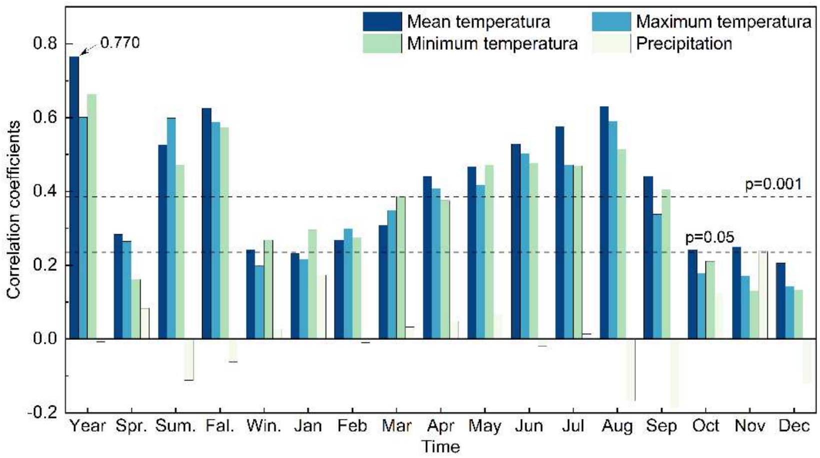

Figure 4 Correlations between the tree ring index of *Picea wilsonii* and meteorological data from 1951 to 2020

2.3 Reconstruction and characteristic analysis of the mean annual temperature

2.3.1 Reconstruction of the mean annual temperature

According to the results of the correlation analysis between tree radial growth and climate, the maximum LW density of *Picea wilsonii* was mainly affected by the mean annual temperature. The scatter plot of the tree ring MXD index and observed mean annual temperature from 1951 to 2020 showed a linear distribution. Therefore, the MXD index and T_{ave} were selected as the independent and dependent variables, respectively, and the linear regression model was used to analyse the mean annual temperature of Xinglong Mountain over the past 220 years (1801~2020), and the reconstruction equation is given as follows:

$$y_i = 2.333X_i + 4.581$$

(r =0.770, N=70, R^2 =0.593, R^2_{adj}=0.593, F =75.278, p <0.0001)

where y_i is the mean annual temperature (°C) of the No. i year, and X_i is the MXD index of the tree ring.

Figure 5 shows a comparison of the reconstructed and measured values of the mean annual temperature. The reconstructed series of mean annual temperature fit well with the measured series, and the temperature fluctuations were generally consistent (Fig. 5a). Fig. 5b further shows the close relationship between instrumentally measured temperature and reconstruction temperature during 1951–2020, with a significant positive correlation between the two. The inspection results of the testing according to period are shown in Table 2. In this test, the series was evenly divided into two periods, i.e., 1951~1985 and 1986~2020, which served as the test period and the calibration period, respectively. During the test period, the error was reduced in each period. Both the RE and the effective coefficient (CE) were positive, and the reduction error (RE) values were both greater than 0.5, indicating that the regression model has good predictive ability(Zeng et al.2022). The sign test of the first-order difference and the sign test of the original value both reached the significance level of 0.01, indicating that the reconstructed series and the measured series have good consistency in terms of the change trend; the correlation coefficient (r) and the mean product (t) both passed the significance test of 0.01, indicating that the two have good correlation. In summary, the reconstruction equation passed all the statistical parameter tests, and the fitting results of the reconstruction series and the measurement series were satisfactory; therefore, the reconstruction equation can be used for the reconstruction of the 1801–2020 mean temperature of Xinglong Mountain.

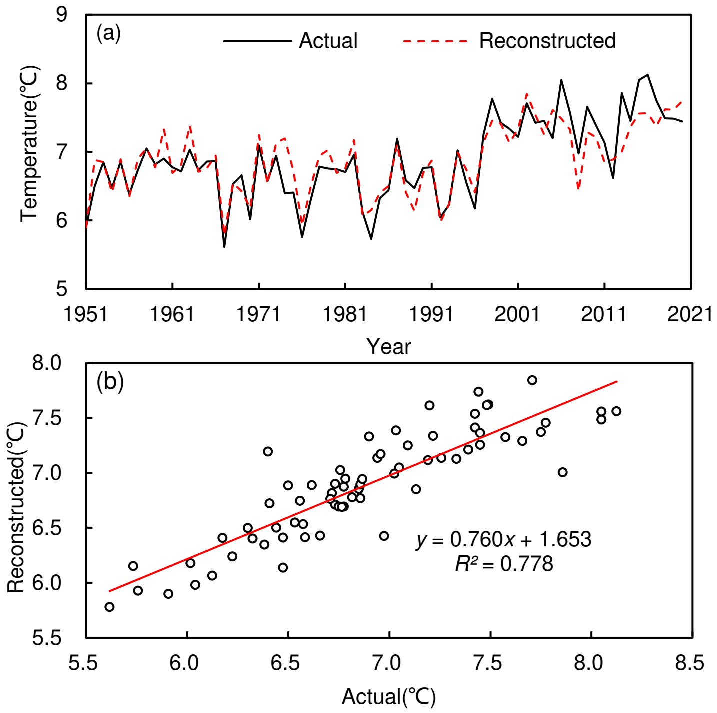

Figure 5 Comparison of the measured and reconstructed mean annual temperatures at the Yuzhong meteorological station

Table 2 Characteristic parameters of the reconstruction equations

	Calibration (1951~1985)	Verification (1986~2020)	Calibration (1986~2020)	Verification (1951~1985)	Calibration (1951~2020)
r	0.662	0.602	0.602	0.662	0.765
R^2	0.437	0.362	0.362	0.437	0.585
CE		0.286		0.230	0.226
RE		0.563		0.531	0.628
ST		32+/3-		28+/7-	58+/12-
ST_1		25+/9-		28+/6-	58+/11-
t		4.504		4.687	7.391
F	40.428		32.433		75.278

2.3.2 Analysis of the characteristics of the reconstructed mean annual temperature series

Figure 5 shows the reconstructed series of the mean annual temperature in the Xinglong Mountains over the past 220 years and the analysis of its temporal variation characteristics. The mean of the reconstructed mean annual temperature series is 6.746°C, and the standard deviation (σ) is 0.607°C. The reconstruction was performed using the Mann–Kendall nonparametric statistical method. A temperature abrupt change test was performed for the series. The results showed that the whole series had abrupt changes in 1811, 1823 and 2008; there were 3 warm periods and 3 cold periods in the whole series, which accounted for 22.73% and 17.27% of the reconstruction years, respectively; and there were 10 extremely cold years and 14 extremely warm years, accounting for 4.55% and 6.36%, respectively, of the whole series.

Fig. 5b shows that after smoothing the mean annual temperature for more than two centuries in the study area, after being smoothed by a 20-year low-pass filter, the reconstruction was completed. The sequence was divided into five periods: abundant, dry, abundant, dry, and abundant. First, from 1801~1817, the mean annual temperature rose rapidly from the normal temperature, and the first abrupt change in the full series occurred during this period, with very warm years occurring sporadically and a significant cycle of 65~70 a; 1817~1855 was the period of temperature decrease. During this period, the coefficient of variation in the mean annual temperature during this period was the largest in the whole series (C_V =0.083). The second abrupt change occurred in the early stage of temperature decline. This period included a longer cold period, which accounted for 26.32% of the cold period years. The duration is 10a, while the extremely cold year is only one year. There was also a significant large-scale cycle of 65~70a, accompanied by the 21~25a mesoscale cycle of the present study. In the second half of the 19th century, the mean annual temperature in the study area was low for the first 20 years, and it was in a cold period between 1857 and 1866; then, the reconstruction temperature rose again, and the multiple warm years concentrated around the early 20th century. Due to the greater degree of series fluctuation in this period (C_V =0.068), the significant large-scale period 65~70a still existed, and the small-scale period 11~16a significantly developed compared with the previous period. From the early 20th century to the present, the reconstructed temperature series did not appear. Therefore, the large-scale significant period disappeared completely, the mesoscale period with a=36~45 gradually became significant, and the reconstructed temperature for the first half of the 20th century began to decline again at a rate of 0.019°C/a and for duration of 42 years. Many extremely cold years appeared in the 1960 s and 1980 s, and they exhibited the longest cold period (18a) in the whole series. Due to the influence of global warming, the reconstructed temperature after the 1980s experienced a third temperature increasing process (C_V =0.073), and a longer warm period and many extremely warm years appeared in the early part of this century, especially during 2010~2020, when there were 10 consecutive warm periods and 2 extremely warm years.

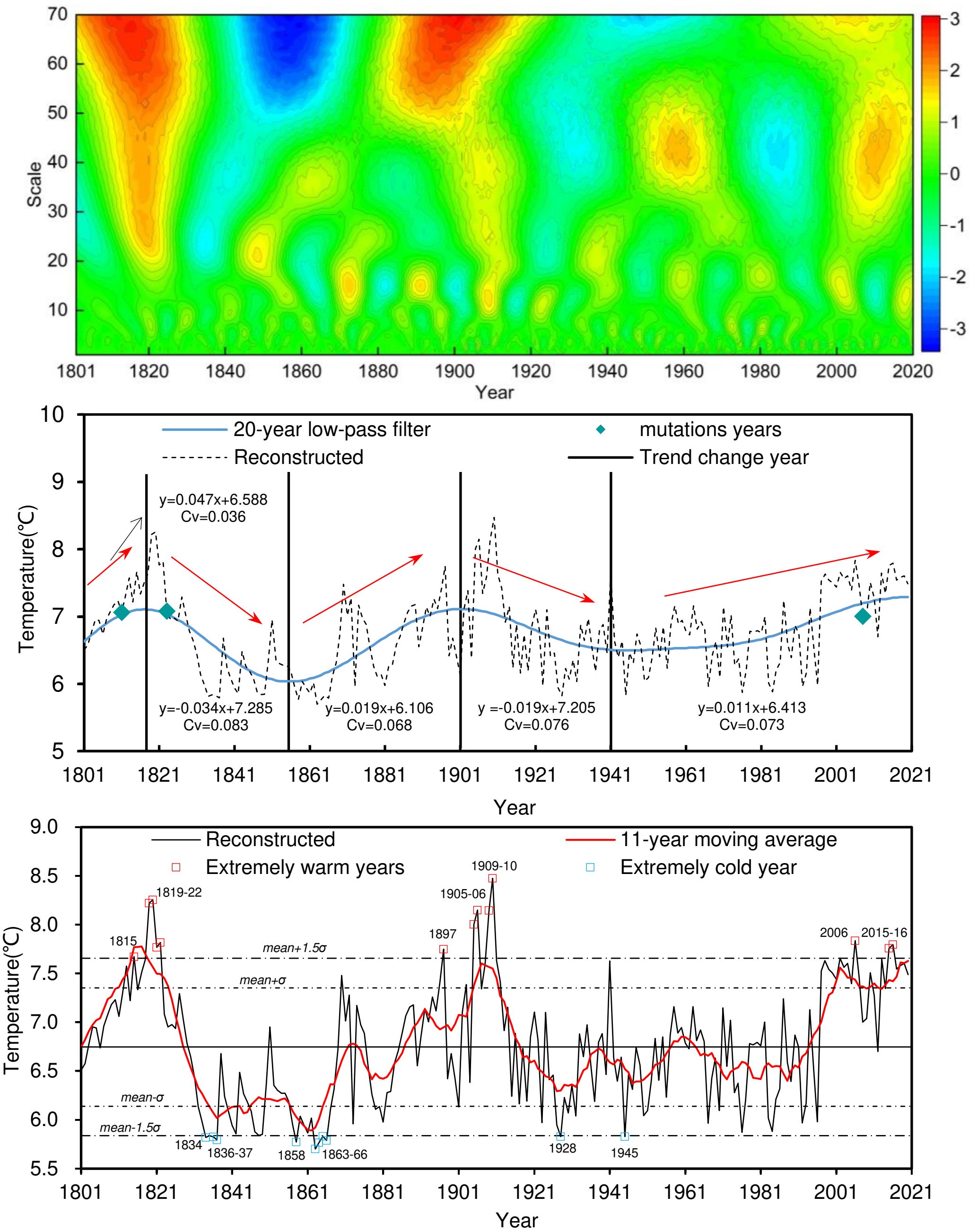

Figure 6 Variation characteristics of the reconstruction series of the mean annual temperature in the Xinglong Mountains area

3. Discussion

3.1 Responses of tree ring density to climatic factors

The MXD of *Picea wilsonii* has different responses to different climatic factors. During July-August, the radial growth of tree cells and the growth of branches and leaves in arid and semiarid areas were basically completed, and the latewood development of the trees began to undergo the photosynthetic accumulation stage. A higher temperature is conducive to the synthesis of photosynthetic substances in trees, provides more nutrients for cell wall thickening, and tends to result in a greater density of late wood(Hartl et al.2022; Rathgeber et al.2016). When the temperature is relatively high from August to September, the available water or water use efficiency of trees decreases. Water scarcity causes the closure of leaf stomata, impairs the radial growth of cells, reduces the demand of trees for photosynthesis, and causes trees to store more photosynthetically. The photosynthetic accumulation of trees mainly acts by thickening the cell walls of latewood cells in tree rings(Chen et al.2019; Römer et al.2021). The study area is part of the typical temperate continental arid climate zone, with hot and dry summers. Therefore, the correlation between the MXD chronology and the temperature in June–August was much greater than that in other months. Although the precipitation is mainly concentrated between June and August, the evaporation during this period is greater due to the higher temperature. Therefore, precipitation has little effect on the MXD during this period (Julio et al.2023). After September, the gradual decrease in temperature and the decrease in sunshine duration cause trees to enter a dormant state. Low temperature will affect the rate of chemical reactions in trees and prevent them from carrying out biological activities, such as photosynthesis(Chen et al.2019; Esper et al.2020). Moreover, a reduction in light time limits the growth and energy acquisition of trees; after winter, the physiological activities of trees nearly stop, and the woody cells in the tree cambium stop dividing(Duan et al.2010) until the spring of the second year; therefore, the correlation between the chronology of the MXD and temperature from October to January of the second year was not significant. This phenomenon was consistent with what has been observed in northern Daxing'sanlings(Sun et al.2012), Southern Tianshan(Li et al.2023) and the Southeastern Qinghai–Tibet Plateau(Li et al.2016).

3.2 Comparison of the reconstructions of the mean annual temperature and the results of other reconstructions

The reliability of the reconstruction results can be verified based on long-term temperature records from adjacent areas and areas at the same latitude. The reconstructed temperature series for the adjacent area is the mean temperature for July reconstructed based on the *Picea crassifolia* width chronology in the eastern Qilian Mountains(Gao et al.2015). The reconstructed temperature series at the same latitude over the past 1000 years were reconstructed based on the *Juniperus przewalskii* width chronology in the central Qilian Mountains(Liu et al.2007); for the same latitude on the Qinghai–Tibet Plateau, reconstructions of the winter minimum temperature and summer maximum temperature for the past 4.5 centuries were constructed based on the common juniper width data(Gou et al.2008).

Five groups of reconstructed series were subjected to 20-year low-pass filter smoothing and cold and warm periods. Overall, the five groups of temperature reconstruction series were all in the temperature decreasing phase during the mid-19th century and the early-to-mid-20th century. With the influence of warming, the five reconstructions since the 1980s were all in the rapid temperature increase phase. However, in the early 19th century, the mean annual temperature in the Xinglong Mountains, the average temperature in July in the eastern part of the Qilian Mountains, and the highest temperature in the summer on the Qinghai–Tibet Plateau all captured this phenomenon of temperature increase, while the mean annual temperature in the central Qilian Mountains and the minimum temperature in the Qinghai–Tibet Plateau in winter slightly decreased during this period. Similarly, from the 1880s to the 1920s, the results of this reconstruction and the mean annual temperature in the central Qilian Mountains showed an upwards trend, with these reconstruction series showing a large degree of variation accompanied by many very warm years. In the two temperature reconstructions of the Qinghai–Tibet Plateau (Figure 7c, d), the warming trend was not shown during this period, while the eastern Qilian Mountains showed a decreasing trend in temperature. These differences may be caused by regional differences and the selection of tree species. These differences are due to differences in reconstruction scale. In summary, the reconstruction results at this time and the reconstruction results for the eastern Qilian Mountains in the adjacent area are roughly the same for both the change trend and the division of cold and warm periods. There are fewer periods with the same division of cold and warm periods as in areas farther away but at the same latitude, but both periods show a trend towards the second half of the 20th century. The warmer leaf temperature characteristics indicate that the reconstruction of the mean annual temperature can reveal the characteristics of climate change in this region.

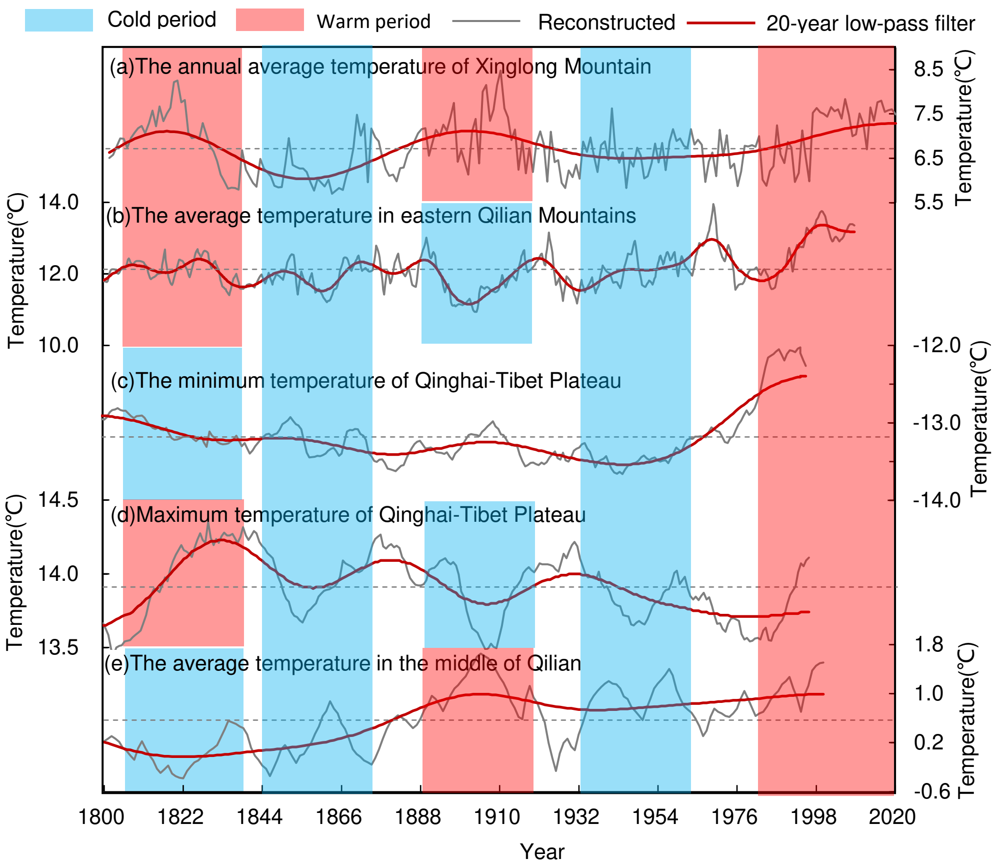

Figure 7 Comparison of these reconstruction results and other reconstruction results

The reliability of the reconstruction results was further validated, and the reconstruction results were compared with those of the Gansu Meteorological Disaster Dictionary(Wen 2005). For comparison, according to historical records, severe cold and frost are important disastrous weather conditions in Gansu Province. In the very cold years and the colder years recorded in this reconstruction, we found that there were multiple years corresponding to them, such as 1833 and 1864. In April 1927, heavy snowfall and frost disasters occurred in Qingyang city, Gansu Province; additionally, the planted grains experienced frost disasters, and grain production decreased. In 1841, March 1863 and September 1863, many places in Gansu Province experienced frost disasters, a large number of crops were damaged, and people were no longer able to survive. In 1842 and May 1928, Tianshui and Lanzhou were both struck by frequent frosts, the autumn harvest was not completed, the farmers' harvests were poor, and there was not enough ground available for grain. In April 1951, the temperature in the central and northwestern regions of Gansu Province was 1~3 °C lower than that in previous years. Wind and snow cooling and frost occurred, and many places experienced severe frost damage. In addition, historical data have recorded warm and cold changes in Gansu Province over the past 5000 years. The climate of Gansu Province is considered to have experienced four warm periods and four cold periods, with a cold period of 1797~1870 and a warm period of 1871~1923. The warm and cold periods recorded in the reconstructed series matched each other. The years with colder temperature reconstructions in the study area all included records of natural disasters, such as snowstorms, cold waves, and frost, which strongly supported the accuracy of the reconstruction results.

3.3 Space representative analysis of the reconstruction series of the mean annual temperature

To test the spatial representativeness of the reconstructed temperature series of the Xinglong Mountains, the CRU TS4.04 grid observation dataset underwent spatial correlation analysis with the observed and reconstructed mean annual temperature series (1951~2020). The results show that the mean annual temperature is the reconstructed series, and the observation series have good spatial consistency. Spatial correlation analysis between the actual measurement series of the mean annual temperature and the corresponding CRU grid points revealed that there was a significant ($p<0.0.5$) correlation field across nearly the entire Qilian Mountains, Xinjiang, and Mongolia, especially near the study area. There was a significant correlation between the two levels (r =0.68, n=70, $p<0.001$). In addition, the spatial correlation between the reconstructed mean annual temperature and the corresponding grid point temperature during 1951–2020 revealed that a significant ($p<0.05$) correlation also covered a large area; however, compared with those in the measured series, the ranges of areas with large correlations were smaller. These results indicate that our reconstruction series can be used to accurately reconstruct the interannual temperature variation during the long historical period in the high-frequency domain of the eastern Qilian Mountains.

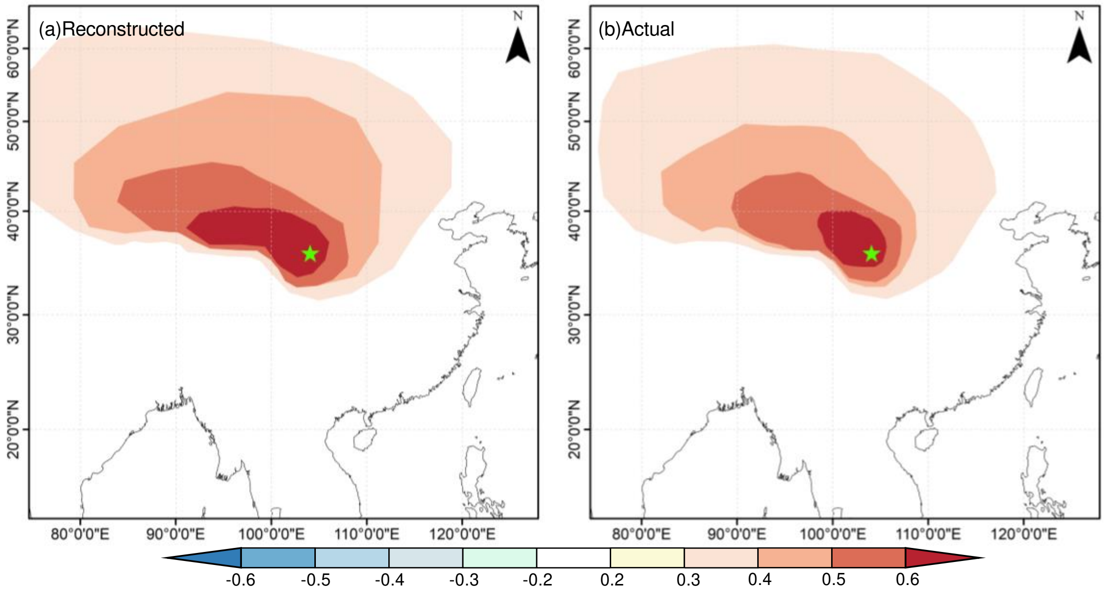

Figure 8 Spatial correlation analysis of the instrumental data and reconstruction data of the 1951–2020

mean annual temperature in the Xinglong Mountain area and the CRU grid data

4 Conclusions

(1) In this study, the chronology of tree ring density data for the years 1765-2020 was established using *Picea wilsonii* , and the correlations between tree ring density and temperature and precipitation were investigated. The analysis results showed that the radial growth of *Picea wilsonii* was closely related to the mean annual temperature (r = 0.77, p<0.001), which has clear physiological significance for trees.

(2) The mean annual temperature series for the Xinglong Mountains between 1801 and 2020 were reconstructed using the *Picea wilsonii* MXD chronology, and the reconstructed series exhibited good reliability (RE=0.728, CE=0.226). The reconstruction results reveal that over the past 200 years, the mean annual temperature in the Xinglong Mountains has experienced 3 warm periods (1813~1822, 1896~1912, 1998~2020) and 3 cold periods (1833~1842, 1857~1866, 1967~1984), and there are also significant cycles of 11~16a, 36~45a, and 65~70a.

(3) The *Picea wilsonii* tree ring density chronology established in this paper has enriched the global tree ring bank. The mean annual temperature series over a long period of time was reconstructed in the Yanshan area (Xinglong Mountain) east of the Qilian Mountains. The spatial representation of regional temperature change has been good, revealing the climate change characteristics of the Xinglong Mountains over the past 200 years, which is helpful for obtaining a better understanding of regional climate change and provides references for future research.

Declarations

Funding information: This research was supported by the National Natural Science Foundation of China [grant numbers 52069019, 52379015 and 51669016] and the Inner Mongolia Autonomous Region “Grassland Talents” project.

Competing Interests: The authors have no relevant financial or non-financial interests to disclose.

Author Contributions: All authors contributed to the study conception and design. Jing Zhang carried out the Conceptualization, Data curation, Formal analysis and Writing - original draft. Bolin Sun, Yingnan Wei and Ziyue Zhang helped in the Investigation and Software. Long Ma provided guidance in the Funding acquisition, Investigation, Methodology and Writing - review and editing. Tingxi Liu helped in Resources, Sample collection and Visualization.

Data Availability: Data are available with the corresponding author.

References

1. Briffa KR, Jones PD, Schweingruber FH, Osborn TJ (1998) Influence of volcanic eruptions on Northern Hemisphere summer temperature over the past 600 years. Nature 393:450–455. https://doi.org/10.1038/30943.
2. Buntgen U, Raible CC, Frank D, Helama S, Cunningham L, et al (2011) Causes and Consequences of Past and Projected Scandinavian Summer Temperatures, 500–2100 AD. PLoS ONE 6(9): e25133. https://doi.org/10.1371/journal.pone.0025133
3. Chao QC, Li RK, Cui T, Wei C (2023) Scientific progress and future prospects in climate change: an interpretation of Part 1 of China's Fourth National Assessment Report on Climate Chang. (in Chinese) China population, resources and environment.
4. Chen F, Yuan YJ, Yu SL, Chen FH (2019) A 391-year summer temperature reconstruction of the Tien Shan, reveals far-reaching summer temperature signals over the midlatitude Eurasian continent. J Geophys Res Atmos 124:11850–11862. https://doi.org/10.1029/2019JD030301.
5. Chen JH, Wang HP, Liu Y, Ma S, Huang W (2023) Temperature variations along the Silk Road over the past 2000 years: Integration and perspectives. Science China Earth Sciences 66(7): 1468–1477. https://doi.org/10.1007/s11430-022-1079-5.
6. Cook ER, Briffa KR, Jones PD (1994) Spatial regression methods in dendroclimatology: a review and comparison of two techniques. International Journal of Climatology14: 379-402. https://doi.org/ 10.1002/joc.3370140404.
7. Cook ER, Holmes RL (1986) Users Manual for ARSTAN: Laboratory of Tree-ring Research. Tucson: University of Arizona 1986:50-60. https://doi.org/10.2172/138036.
8. Duan J P, Wang L, Li L, Chen KL (2010) Temperature variability since A.D. 1837 inferred from tree-ring maximum density of Abies fabri on Gongga Mountain, China. Chinese Sci Bull 55: 3015−3022, https://doi.org/10.1007/s11434-010-3182-8.
9. Esper J, George SS, Anchukaitis K, D'Arrigo RD, Ljungqvist FC, Luterbacher J, Schneider L, Stoffel M, Wilson R, Büntgen U (2018) Large-scale, millennial temperature reconstruction from tree rings. Dendrochronologia 50:81–90. https://doi.org/10.1016/j.dendro.2018.06.001
10. Esper J, Klippel L, Krusic PJ, Konter O, Raible CC, Xoplaki E, Luterbacher J, Büntgen U (2020) Eastern Mediterranean summer temperatures since 730 CE from Mt. Smolikas tree-ring densities. Clim Dyn 54, 1367–1382. https://doi.org/10.1007/s00382-019-05063-x.

11. Franke J, Frank DC, Raible CC, Esper J (2013) Spectral biases in treering climate proxies. Nat Clim Change 3:360–364.

12. Gao LL, Gou XH, Deng Y, Yang MX, Zhang F, Li J (2015) Dendroclimatic reconstruction of temperature in the eastern Qilian Mountains, northwestern China. Climate research 62: 241–25. https://doi.org/10.3354/cr01271.

13. Gou XH, Chen FH, Yang MX, Jacoby G, Fang KY, Tian QH, Zhang Y (2008) Asymmetric variability between maximum and minimum temperatures in Northeastern Tibetan Plateau: Evidence from tree rings. Science in China Series D: Earth Sciences 51:41-55. https://doi.org 10.1007/S11430-007-0154-1.

14. Gou XX, Zhang TW, Yu SL, Liu KX, Zhang RB, Shang HM, Qin L, Fan YT, Jiang SX, Zhang HL, Guo D (2023) Climate response of Picea schrenkiana based on tree-ring width and maximum density. Dendrochronologia Volume 78, 2023, 126067. https://doi.org/10.1016/j.dendro.2023.126067.

15. Hartl C, Schneider L, Riechelmann DFC, Eileen K, Markus K, Lara K, Ulf B, Jan E (2022) The temperature sensitivity along elevational gradients is more stable in maximum latewood density than tree-ring width. Dendrochronologia 73:125958. https://doi.org/10.1016/j.dendro.2022.125958

16. Hartl C, Schneider L, Riechelmann DFC, Kuhl E, Kochbeck M, Klippel L, Büntgen U, Esper J (2022) The temperature sensitivity along elevational gradients is more stable in maximum latewood density than tree-ring width. Dendrochronologia 73:125958-. https://doi.org/10.1016/j.dendro.2022.125958.

17. He YL, Ding L, Li DD, Huang JP, Li CY, Mi L (2019) Research Review on the Contrast of Land and Ocean Warming Features Under the Global Warming. (in Chinese) Journal of Arid Meteorology.

18. Hennessy K, Lawrence J, Mackey B (2022) IPCC sixth assessment report (AR6): climate change 2022impacts, adaptation and vulnerability: regional factsheet Australasia.

19. Holmes, Richard L (1983) Computer-Assisted Quality Control in Tree-Ring Dating and Measurement. Tree-Ring Bulletin 43:51-67. http://hdl.handle.net/10150/261223.

20. Jiao L, Xue R, Qi CL, Chen K, Liu XP (2021) Comparison of the responses of radial growth to climate change for two dominant coniferous tree species in the eastern Qilian Mountains, northwestern China. International Journal of Biometeorology 65: 1823-1836. https://doi.org/10.1007/s00484-021-02139-4.

21. Jiao L, Xue RH, Qi CL, Chen K, Liu XP (2021) Comparison of the responses of radial growth to climate change for two dominant coniferous tree species in the eastern Qilian Mountains, northwestern China. International Journal of Biometeorology 2021:1-14. https://doi.org/10.1007/s00484-021-02139-4.
22. Julio Camarero J (2023) Imprints of climate stress on tree growth (the past as harbinger of the future): ecological stress memory in Tibetan Plateau juniper forests. Proceedings of the Royal Society B 290(1992): 20222241.
23. Keyimu M, Li ZS, Zhang GS, Fan ZX, Wang XC, Fu BJ (2020) Tree ring–based minimum temperature reconstruction in the central Hengduan Mountains, China. Theoretical and Applied Climatology. https://doi.org/10.1007/s00704-020-03169-5
24. Khasanov BF, Karpukhin AA, Krenke NA, Pevzner MM, Tarabardina OA, Vasyukov DD, Yermokhin MV, Savinetsky AB (2021) Long oak tree-ring chronologies from CentralRussia and their potential for dating. Tree-Ring Research 77(2): 53-62. https://doi.org/10.3959/TRR2020-5.
25. Li MQ, Huang L, Yin ZY. Shao XM (2016) Temperature reconstruction and volcanic eruption signal from tree-ring width and maximum latewood density over the past 304 years in the southeastern Tibetan Plateau. Int J Biometeorol 61, 2021–2032. https://doi.org/10.1007/s00484-017-1395-0.
26. Li P, Song HM, Liu Y, Zhang Q, Fang CX, Li Q, Cai QF, Zeng XL, Ma YF (2023) Maximum July–August temperatures for the middle of the southern Tien Shan inferred from tree-ring latewood maximum densities. Int J Biometeorol 67, 321–335. https://doi.org/10.1007/s00484-022-02408-w.
27. Liu LY, Gou XH, Zhang F, Yin DC, Wang XJ, Xia JQ, Li Q, Du MM (2021) Effects of warming on radial growth of Picea crassifolia in the eastern Qilian Mountains, China. (in Chinese) Chinese Journal of Applied Ecology.
28. Liu XH, Shao XM, Zhao LJ, Qin DH, Chen T, Ren JW (2007) Dendroclimatic Temperature Record Derived from Tree-Ring Width and Stable Carbon Isotope Chronologies in the Middle Qilian Mountains, China. Arctic Antarctic, and Alpine Research 39(4):651-657. http://dx.doi.org/10.1657/1523-0430(07-506)[LIU-X]2.0.CO;2
29. Liu Y, Wang L, Li Q, Cai QF, Song HM, Sun CF, Liu RS, Mei RC (2019) Asian summer monsoon-related relative humidity recorded by tree ring δ 18 O during last 205 years. Journal of Geophysical Research: Atmospheres 124, 9824–9838.https://doi.org/10.1029/2019JD030512

30. Luckman BH, Wilson RJS (2005) Summer temperatures in the Canadian Rockies during the last millennium: a revised record. Climate Dynamics 24:131–144. https://doi.org/10.1007/s00382-004-0511-0.
31. Nunes LJR, Ferreira Dias M (2022) Perception of Climate Change Effects over Time and the Contribution of Different Areas of Knowledge to Its Understanding and Mitigation. Climate 10(1): 7-18. https://doi.org/10.3390/cli10010007.
32. Rathgeber CBK, Cuny HE, Fonti P (2016) Biological basis of tree-ring formation: a crash course. Front Plant Sci 7:1–7. https://doi.org/10.3389/fpls.2016.00734.
33. Römer P, Hartl C, Schneider L, Bräuning A, Szymczak S, Huneau F, Lebre S, Reinig F, Büntgen U, Esper J (2021) Reduced temperature sensitivity of maximum latewood density formation in high-elevation Corsican Pines under recent warming. Atmosphere 12:804. https://doi.org/10.3390/atmos12070804.
34. Sun Y, Wang LL, Chen J, Duan JP (2012) Reconstructing mean maximum temperatures of May–August from tree-ring maximum density in North Da Hinggan Mountains, China. (in Chinese) Chin Sci Bull 57: 2007–2014. https://doi.org/ 10.1007/s11434-012-5055-9.
35. Tian QH, Zhou XJ, Gou XH, et al (2012) Analysis of reconstructed annual precipitation from tree-rings for the past 500 years in the middle Qilian Mountain. Sci China Earth Sci 55: 770–778, https://doi.org/10.1007/s11430-012-4375-6.
36. Timothy JO, Keith RB, Fritz HS, Phil DJ (2004) Annually resolved patterns of summer temperature over the Northern Hemisphere since AD 1400 from a tree- ring-density network.
37. Uttam P, Takeshi N, Nivedita M, Li Z, Yoshikazu K, Masaki S, Santosh KS (2023) Tree-rings stable isotope (δ18O and δ2H) based 368 years long term precipitation reconstruction of South Eastern Kashmir Himalaya, Science of The Total Environment, Volume 892, 164640. http://dx.doi.org/10.1016/j.scitotenv.2023.164640
38. Venugopal V, Foufoula-Georgiou E (1996) Energy decomposition of rainfall in the time-frequency-scale domain using wavelet packets. Journal of Hydrology 187(1-2), 3-27.
39. Wang S, Jiao L, Jiang Y, Liu XR, Chen K, Liu XP (2022) Tree-ring-based drought-pluvial variation in the Tianshan Mountains of northwestern China. Theoretical and Applied Climatology 148:1727–1740. https://doi.org/10.1007/s00704-022-04028-1.
40. Wang T, Bao A, Xu WQ, Yu RD, Zhang QL, Jiang LL, Nzabarinda V (2021) Tree-ring-based

assessments of drought variability during the past 400 years in the Tianshan mountains, arid Central Asia. Ecological Indicators 126[2024-02-28]. https://doi.org/10.1016/j.ecolind.2021.107702

41. Wang XJ, Pang GJ, Yang MX, Wan GN, Liu ZC (2018) Precipitation changes in the Qilian Mountains associated with the shifts of regional atmospheric water vapour during 1960 − 2014. International Journal of Climatology 38:4355 − 4368. https://doi.org/10.1002/joc.5673.
42. Wang ZG, Ji DR, Feng TJ (2017) China's economic trees. 3. (in Chinese) Northeast Forestry University Press.
43. Wen KG (2005) China meteorological disaster ceremony, Gansu roll. (in Chinese) China Meteorological Pres.
44. Xia J, Ning L, Wang Q, Chen JX, Wan L, Hong S (2017) Vulnerability of and risk to water resources in arid and semi-arid regions of West China under a scenario of climate change. Climatic Change 144: 549 − 563. https://doi.org/10.1007/s10584-016-1709-y.
45. Yang D, Yang Y, Xia J (2021) Hydrological cycle and water resources in a changing world: A review. Geography and Sustainability 2(2): 115-122. https://doi.org/10.1016/j.geosus.2021.05.003.
46. Zachary G, Amy H, Kevin A, Shikha S, Michael NE, Scott N (2022) Investigating the potential for Southern Hemisphere climate reconstruction using stable isotopes in Tasmanian tree rings. Dendrochronologia Volume 76, 126016. https://doi.org/10.1016/j.dendro.2022.126016.
47. Zeng X, Liu Y, Song H, Li Q, Cai QF, Fang CX, Sun CF, Ren M (2022) Tree-ring-based drought variability in northern China over the past three centuries. Journal of Geographical Sciences 32(2):214-224. https://doi.org/10.1007/s11442-022-1943-3.
48. Zhang F, Chen Q, Gou XH, Du MM, Wang F, Zhang JZ (2021) Climatic control on the growth and regeneration of Juniperus przewalskii at alpine treeline in the eastern Qilian Mountains, northwest China. Trees 35: 1085-1097. https://doi.org/10.1007/s00468-021-02123-w.
49. Zhang Y, Shao X, Wilmking M (2011) Dynamic relationships between Picea crassifolia growth and climate at upper treeline in the Qilian Mts. Northeast Tibetan Plateau, China. Dendrochronologia 29(4):185-199. https://doi.org/10.1016/j.dendro.2010.11.001.
50. Zhao YJ, Keyimu M, Li ZS, Chen YZ, Wei JS, Wang XC, Fan ZX (2021) Summer mean temperature reconstruction during the past 285 years based on tree-ring in northern Gaoligong Mountains, northwestern Yunnan of China. Geografiska Annaler: Series A, Physical Geography. https://doi.org/10.1080/04353676.2020.1854012.

51. Zheng T, Jordi MV, Raúl GV, Antonio G, Julio C, Ma CC M, Maurizio M (2023) Growth plasticity of conifers did not avoid declining resilience to soil and atmospheric droughts during the 20th century. Forest Ecosystems 10(2):238-251. https://doi.org/10.1016/j.fecs.2023.100107